Supplementary Materials

Dae-Yeon Jo[#], Hyun-Min Kim[#], Goo Min Park, Donghyeok Shin, Yuri Kim, Yang-Hee Kim, Chae Woo Ryu[*], Heesun Yang[*]

Department of Materials Science and Engineering, Hongik University, Seoul 04066, Republic of Korea.
[#]Authors contributed equally.

[*]**Correspondence to:** Prof. Heesun Yang, Prof. Chae Woo Ryu, Department of Materials Science and Engineering, Hongik University, 94, Wausan-ro, Mapo-gu, Seoul 04066, Republic of Korea. E-mail: hyang@hongik.ac.kr; cryu@hongik.ac.kr

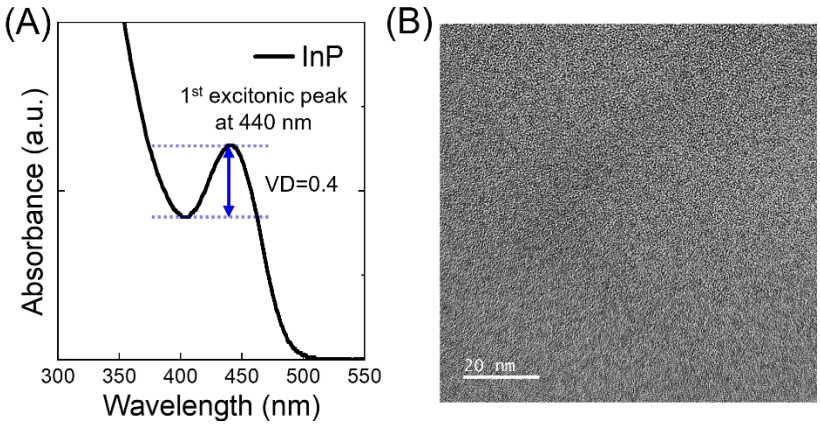

Supplementary Figure 1. (A) Absorption spectrum and (B) TEM image (scale bar: 20 nm) of green-emissive InP cores.

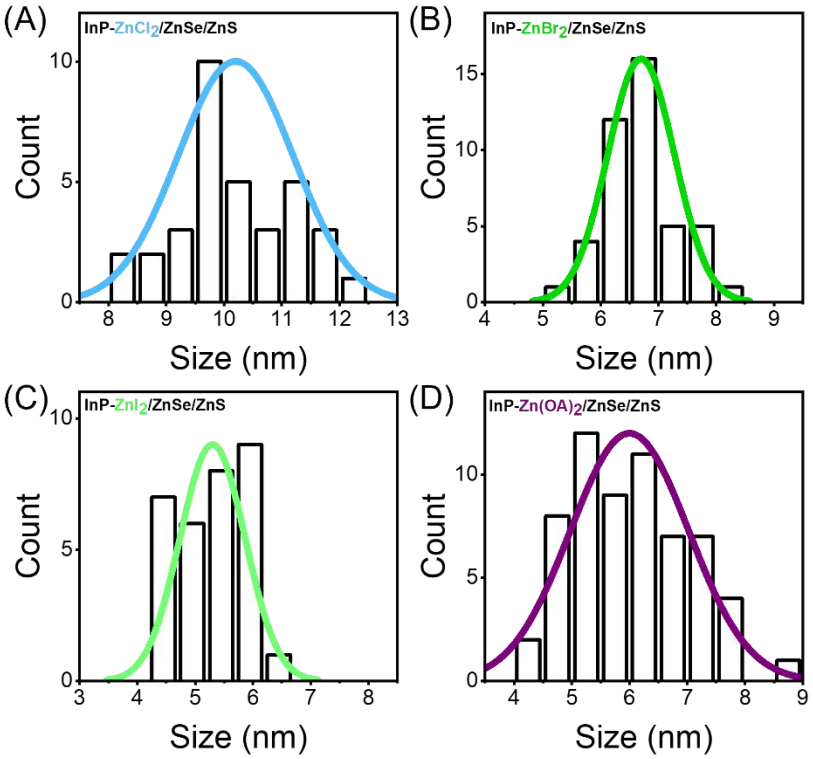

Supplementary Figure 2. Size distribution histograms of InP/ZnSe/ZnS QDs synthesized with different Zn precursor types of (A) $ZnCl_2$, (B) $ZnBr_2$, (C) ZnI_2 and (D) $Zn(OA)_2$, which were derived from Figure 1C–F, respectively.

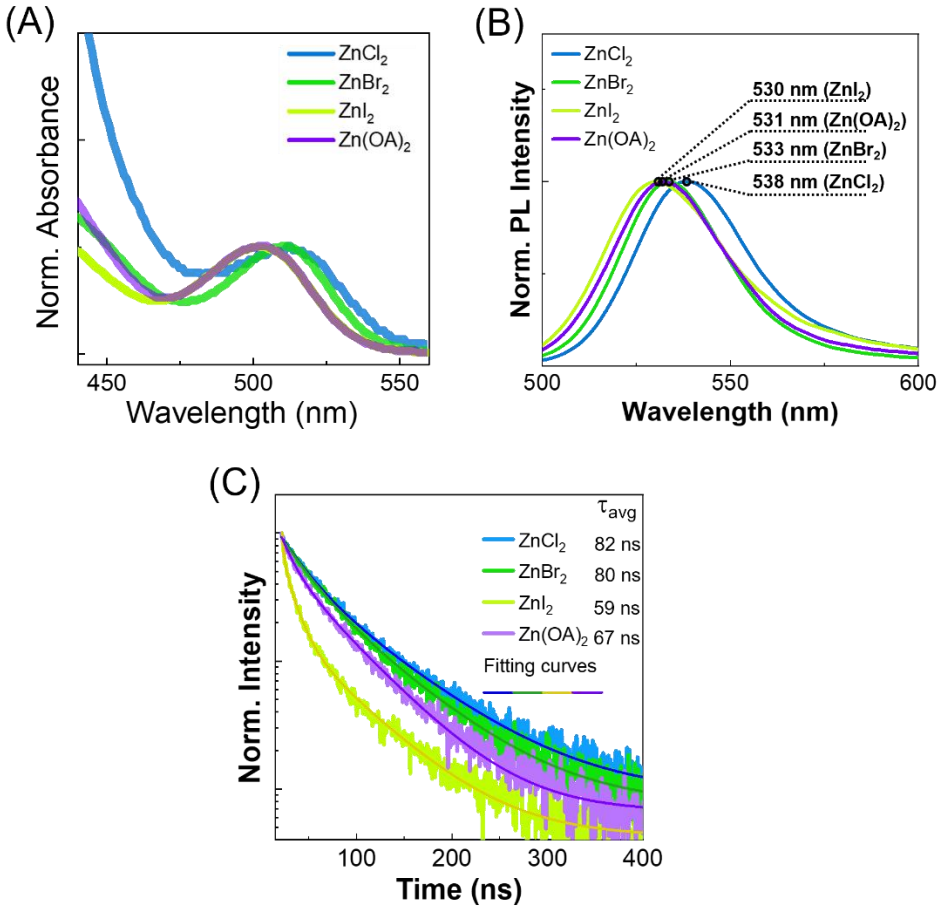

Supplementary Figure 3. (A) Normalized absorption (magnified from Figure 1B), (B) PL spectra and (C) time-resolved PL decay profiles of InP/ZnSe/ZnS QDs synthesized with different Zn precursor types of ZnX_2 (X = Cl, Br, I) and $Zn(OA)_2$ for growth of ZnSe inner and ZnS outer shell.

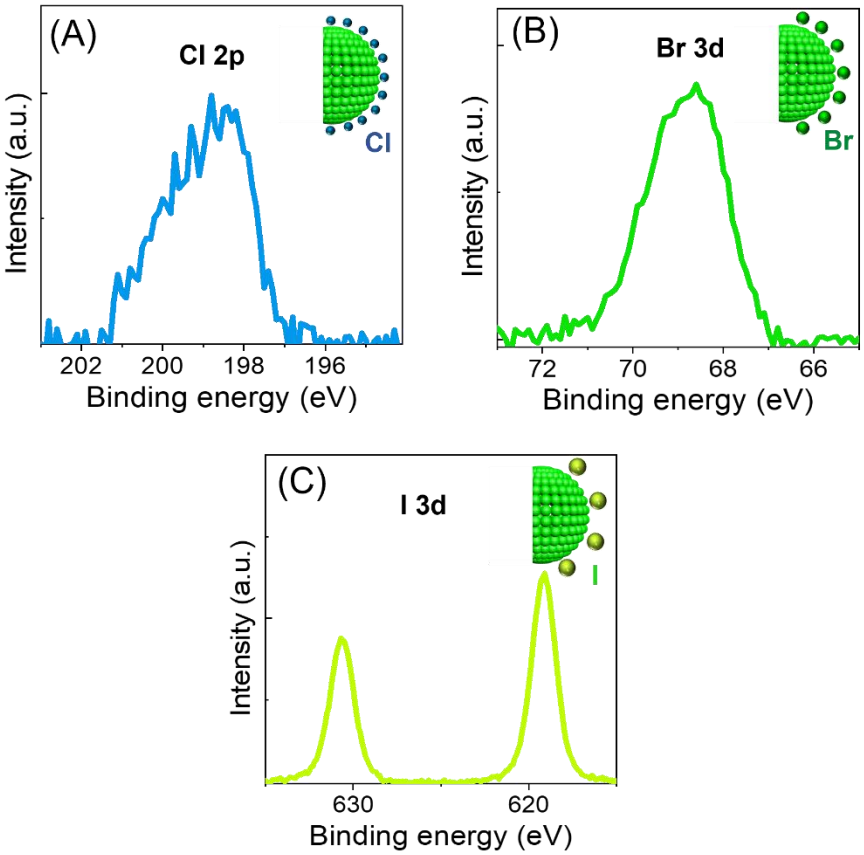

Supplementary Figure 4. (A) Cl 2p, (B) Br 3d, and (C) I 3d XPS spectra of a set of InP-ZnX_2-$Zn(OA)_2$ cores, where X = Cl, Br, and I, respectively.

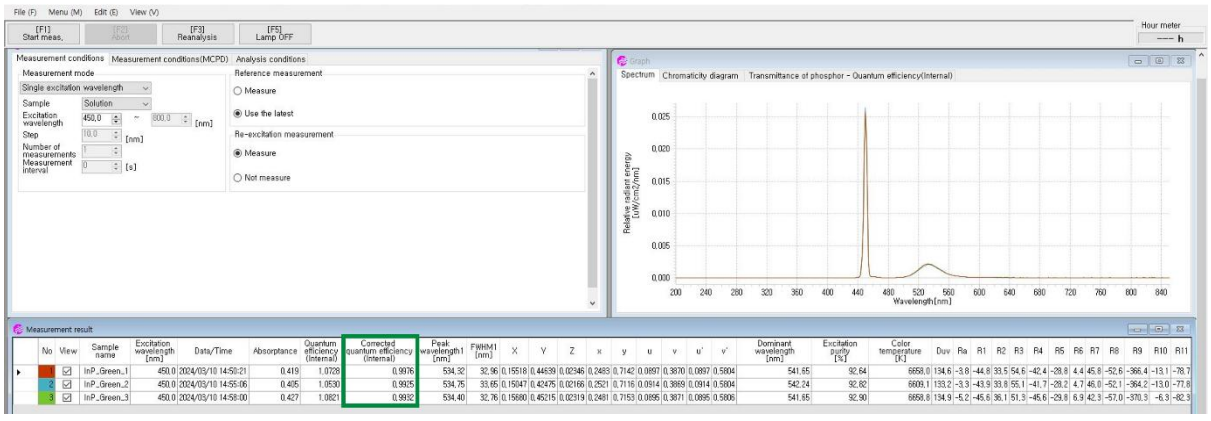

Supplementary Figure 5. Screen shot image of PL measurement results from the representative three InP-$ZnBr_2$-$Zn(OA)_2$/ZnSe/ZnS QD samples showing PL QYs of 99.25%–99.76%.

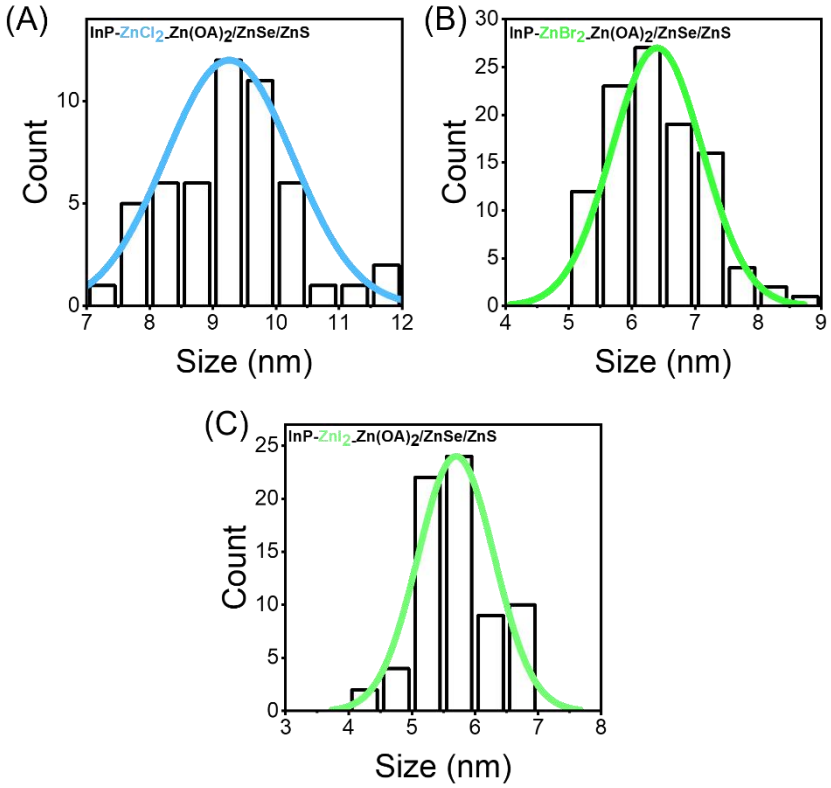

Supplementary Figure 6. Size distribution histograms of InP-ZnX_2-$Zn(OA)_2$/ZnSe/ZnS QDs, where ZnX_2 is (A) $ZnCl_2$, (B) $ZnBr_2$, and (C) ZnI_2, which were derived from Figure 4A–C, respectively.

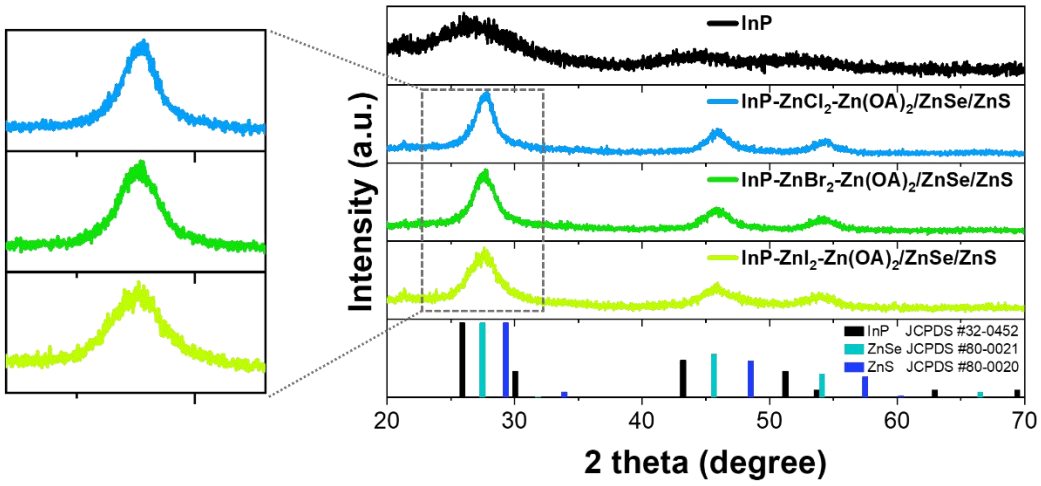

Supplementary Figure 7. XRD patterns of InP cores and a series of InP-ZnX_2-$Zn(OA)_2$/ZnSe/ZnS QDs.

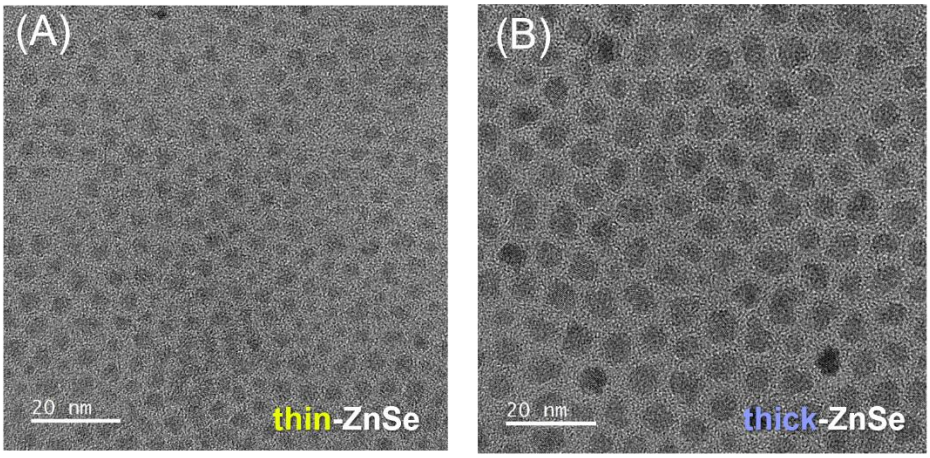

Supplementary Figure 8. TEM images (scale bar: 20 nm) of InP-$ZnBr_2$-$Zn(OA)_2$/ZnSe QDs having (A) thin- and (B) thick-ZnSe.

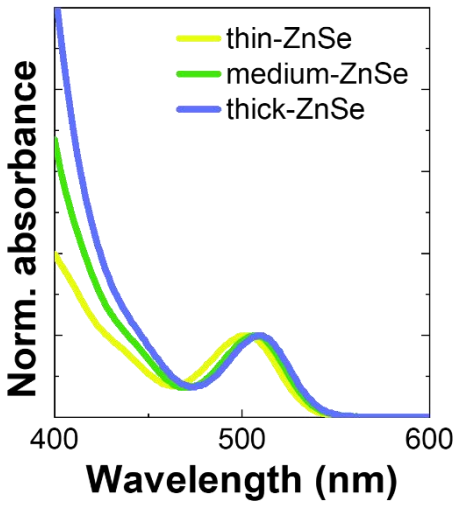

Supplementary Figure 9. Absorption spectra normalized at the 1S peak of InP-$ZnBr_2$-$Zn(OA)_2$/ZnSe/ZnS QDs with different ZnSe inner shell thicknesses.

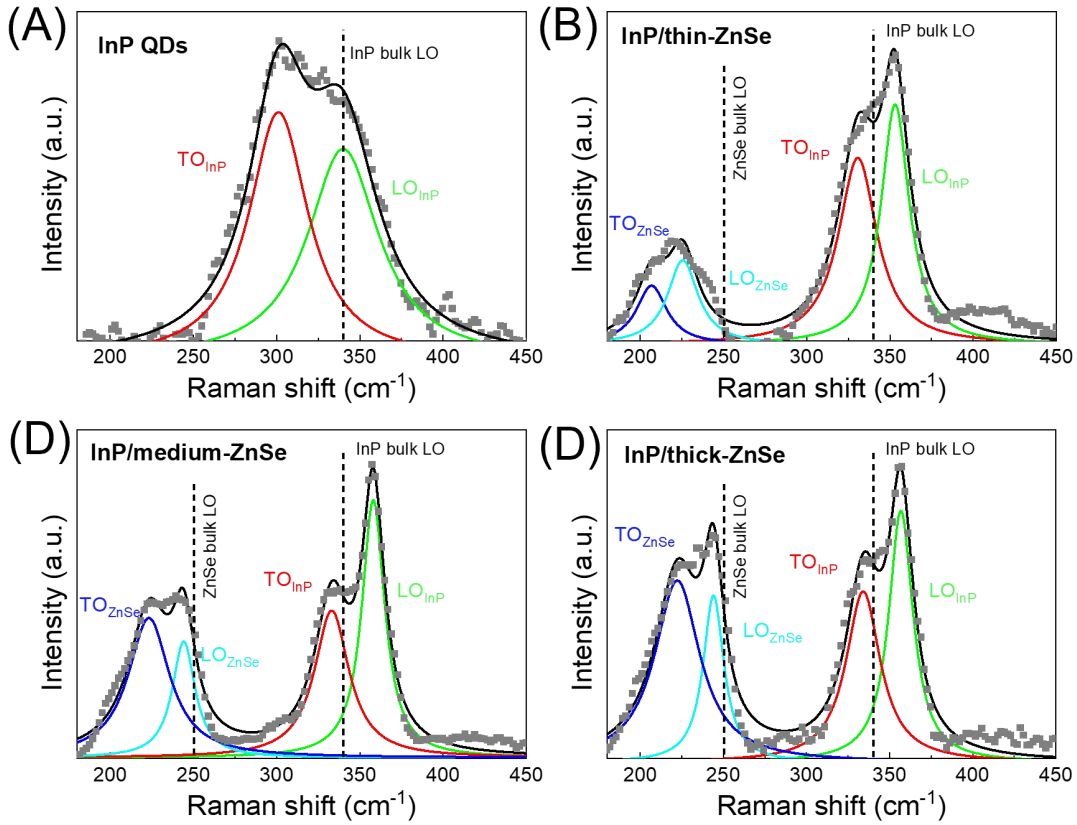

Supplementary Figure 10. Raman spectra of (A) InP cores and a series of InP-$ZnBr_2$-$Zn(OA)_2$/ZnSe QDs having (B) thin-, (C) medium-, and (D) thick-ZnSe shell. The vertical dotted lines present the reference wavenumbers for InP and ZnSe bulk LO modes, as indicated. The Lorentz function was applied to determine the sub-bands widths and center frequencies for quantitative Raman analysis.

Supplementary Table 1. Summarized quantitative values obtained by Raman analysis in Supplementary Figure 8

	TO ZnSe	LO ZnSe	TO InP	LO InP	Strain_InP	Strain_ZnSe
Core	-	-	301.1	340.0	0.00	-
Thin-ZnSe	206.8	226.8	330.7	353.0	-0.99	4.05
Medium-ZnSe	220.6	244.1	334.3	358.1	-1.37	0.95
Thick-ZnSe	224.2	246.0	336.0	358.7	-1.41	0.64

The sub-bands correspond to LO and transverse optical phonon (TO) modes of InP and ZnSe [1–5]. The center frequencies of TO and LO in each band of InP and ZnSe are also listed in Table S1. The Raman spectrum of InP core is characterized by two modes of TO (301.1 cm^{-1}) and LO (340 cm^{-1}). Upon increasing thickness of ZnSe shell on InP core, the LO of InP shifted to a higher frequency along with appearance of ZnSe band. Meanwhile, as ZnSe shell became thicker, LO of ZnSe gradually moved toward its bulk LO value with the signal more intense and narrower [2,4]. The frequency shift ($\Delta\omega/\omega$), obtained from the LO center frequencies in Table S1, can be related to the relative lattice constant change ($\Delta a/a$) by the following equation [1,2,4].

$$\frac{\Delta\omega}{\omega} = \left(1 + 3\frac{\Delta a}{a}\right)^{-\gamma} - 1$$

In this equation, $\gamma = \frac{\partial ln\omega}{\partial lnV}$ is the Grüneisen parameter, where V is the crystal unit cell volume. For the LO mode, the Grüneisen parameters are 1.24 for InP and 0.85 for ZnSe [2,4].

REFERENCES

1. Rafipoor M, Dupont D, Tornatzky H, et al. Strain engineering in InP/(Zn,Cd)Se core/shell quantum dots. Chem Mater 2018;30:4393–4400. **DOI** 10.1021/acs.chemmater.8b01789

2. Rafipoor M, Tornatzky H, Dupont D, et al. Strain in InP/ZnSe, S core/shell quantum dots from lattice mismatch and shell thickness—material stiffness influence. J Chem Phys 2019;151:154704. **DOI** 10.1063/1.5124674

3. Lange H, Kelley DF. Spectroscopic effects of lattice strain in InP/ZnSe and InP/ZnS nanocrystals. J Phys Chem C 2020;124:22839–22844. **DOI** 10.1021/acs.jpcc.0c07145

4. Avermaet HV, Schiettecatte P, Hinz S, et al. Full-spectrum InP-based quantum dots with near-unity photoluminescence quantum efficiency. ACS Nano 2022;16:9701–9712. **DOI** 10.1021/acsnano.2c03138

5. Brodu A, Ballottin MV, Buhot J, et al. Exciton fine structure and lattice dynamics in InP/ZnSe core/shell quantum dots. ACS Photonics 2018;5:3353–3362. **DOI** 10.1021/acsphotonics.8b00615